ELSEVIER

Journal of Power Sources 56 (1995) 11–17

JOURNAL OF POWER SOURCES

A study of heat and material balances in an internal-reforming molten carbonate fuel cell

Y. Miyake [a], N. Nakanishi [a], T. Nakajima [a], Y. Itoh [a], T. Saitoh [a], A. Saiai [b], H. Yanaru [c]

[a] *New Materials Research Center, Sanyo Electric Co., Ltd., 1-1 Dainichi-Higashimachi, Moriguchi City, Osaka 570, Japan*

[b] *Corporate Research & Development Laboratory, Tonen Corporation, 1-3-1 Nishi-Tsurugaoko, Ohimachi, Iruma Gun, Saitama 354, Japan*

[c] *Technology Research Center, Toyo Engineering Corporation, 1818 Togo-Fujimi, Mobara City, Chiba 297, Japan*

Received 20 December 1994; accepted 6 February 1995

Abstract

A study is made of the heat and material balances in internal-reforming, molten carbonate fuel cells. A 5 kW class, indirect internal-reforming molten carbonate fuel cell stack together with a 10 kW class, direct internal-reforming molten carbonate fuel cell stack have been assembled and tested to evaluate the performance, and to obtain basic data on the material and heat balances, in order to assist system design. The input and output heat flux of the stacks are obtained independently, and are in good agreement. Using these procedures, it will be possible to improve the design of internal-reforming, molten carbonate fuel cell systems for co-generation.

Keywords: Molten carbonate fuel cells; Heat balance; Material balance

1. Introduction

The internal-reforming molten carbonate fuel cell (MCFC) is receiving a great deal of attention by virtue of its high efficiency and simple system configuration. In the case of MCFCs used for co-generation purposes, it is very important to evaluate the heat flux around the stack in order to design the most suitable system.

The authors have conducted research on MCFC stacks and systems. In 1990, a 10 kW class, naphtha-fueled, external-reforming, MCFC system was demonstrated successfully [1]. A 30 kW class direct, internal-reforming MCFC system is being tested in order to evaluate the feasibility of the petroleum-fueled MCFC for co-generation applications [2,3].

This paper presents a study of both the material balance and the heat balance in an internal-reforming MCFC around the stacks, and considers the feasibility of applying the system to co-generation service.

2. Experimental

A 5 kW class, indirect internal-reforming MCFC (IIR-MCFC) stack, and a 10 kW class, direct internal-reforming MCFC (DIR-MCFC) stack were assembled and tested.

The key specifications of these stacks are given in Table 1. The 5 kW IIR-MCFC consisted of 21 cells and 4 reforming units (RUs). Fig. 1 shows the construction of the stack. The RUs were situated every 5 cells, and both the top and the bottom end-blocks had 3 cells, respectively. Fuel was supplied from one corner of each RU. The fuel was reformed in the RUs. The fuel went through these RUs, returned to the other end of the RUs, and came out at the anode inlet manifold. Oxidant was supplied from one side of the stack and exited from the anode inlet side. The active area of the electrodes was 2400 cm^2. The 10 kW, DIR-MCFC stack consisted of 27 cells and the electrode area was 4510 cm^2. The reforming catalyst (ZrO_2-based ruthenium) was loaded in the web of the anode gas channel [4]. The gas-flow direction was a cross-flow configuration. The 10 kW, DIR-MCFC stack was made for pre-testing a 30 kW co-generation system. A schematic of the flow in the latter system is presented in Fig. 2 [2]. The system has both the anode and the cathode gas-recycle lines to control the stack temperature, as well as a CO_2-recycle line to recover the CO_2 from the anode outlet so that it may be used for the cathode-reactant gas. In addition, both the anode and the cathode recycle lines have heat exchangers to recover the heat for co-generation. The pressure drop of the heat exchanger causes a pressure (~ 200 mm H_2O) at the stack that is slightly higher than atmospheric pressure. The stack is covered by a vessel which is purged by nitrogen gas to prevent gas leakage from the sealing part of the manifold.

SSDI 0378-7753(95)02199-Q

Table 1
Key specifications of 5 kW and 10 kW class MCFC stacks

Items	5 kW IIR-MCFC stack	10 kW DIR-MCFC stack
Effective cell area (cm^2)	2400	4510
Number of cells	21	27
Rated output power (kW, d.c.)	5	10
Reforming method	in-direct, internal	direct, internal
Reforming unit number	4	
Reforming catalyst	Ni/MgO	Ru/ZrO_2
Operating temperature (°C)	650	650
Operating pressure (atm)	1	1
Anode material	Ni–Al	Ni–Al
Cathode material	NiO	NiO
Matrix material	$LiAlO_2$	$LiAlO_2$
Electrolyte	Li_2CO_3/K_2CO_3 (62/38 mol%)	Li_2CO_3/K_2CO_3 (62/38 mol%)

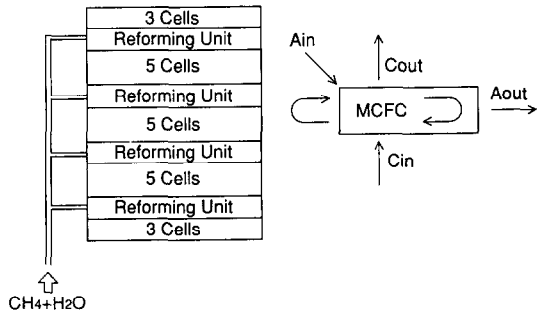

Fig. 1. Construction of 5 kW IIR-MCFC stack.

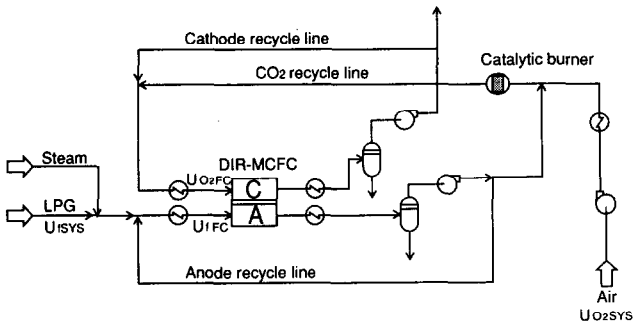

Fig. 2. Schematic flow of 30 kW DIR-MCFC system for co-generation.

Table 2
Standard operating gas composition

Anode gas composition	68 H_2/17 CO_2/15 H_2O
Cathode gas composition	70 air/30 CO_2
Fuel utilization (%)	60–80
Oxidant (O_2 and CO_2) utilization (%)	20

The anode was made from nickel–aluminum alloy powder (Mitsubishi Materials Co., Ltd.). The plaque for cathode was prepared by sintering nickel powder (Inco 287) and oxidizing this to NiO during the stack heat-up procedure to 650 °C. The matrix was composed of $LiAlO_2$ (Foote Minerals Co., Ltd.) and was fabricated by the tape-casting method.

The MCFC stacks were both operated under standard gas and simulated system gas conditions. The standard gas composition is given in Table 2. CH_4 was used as a simulated fuel for the 5 kW IIR-MCFC stack, and LPG-based simulated fuel for the 10 kW DIR-MCFC stack. The system gas composition for the 10 kW DIR-MCFC stack is given in Table 3 [5].

The inlet and outlet gas compositions were measured by gas chromatography. The gas and stack temperatures were measured by type K thermocouples. The gas temperature had to be calibrated, because the measured values were affected by both convection and thermal radiation. The thermocouple was situated in the gas channel near to the rib of the channel. Consequently, the thermal radiation from the gas channel was sufficient and the gas was heated up by the rib of the gas channel so that it was not necessary to calibrate the temperature measured by the thermocouple. On the other hand, the measurement values of the inlet and outlet gas temperatures at the manifolds were affected by the wall of the piping and the surface of the stack as these had high thermal radiation. Accordingly, the calibration was achieved by the following method. In the piping, the thermal balance of the thermocouple is as follows:

$$h_c(T_c - T_g) = \sigma\epsilon(T_w^4 - T_c^4) \quad (1)$$

where h_c is the gas heat-transfer coefficient (W m^{-2} K), T_c the value measured by the thermocouple (K), T_g the real gas temperature (K), T_w the temperature of the piping wall (K), σ the Stefan–Boltzmann constant ($\sigma = 5.67 \times 10^{-8}$ W m^{-2} K^{-4}), and ϵ the emmissivety.

Table 3
Simulated system gas condition for 10 kW DIR-MCFC based on LPG

Anode gas composition	8.4 H_2/46.1 CO_2/5.7 C_3H_8/39.8 H_2O	
Cathode gas composition	9.1 O_2/75.1 N_2/12.4 CO_2/7.0 H_2O	
Anode recycle ratio	0.42	
Cathode recycle ratio	0.75	
Fuel utilization (%)	70 (stack)	80 (system)
Oxidant utilization	27 (stack)	60 (system)
O_2 (%)		
CO_2 (%)		

On substituting the emmissivety heat-transfer coefficient h_r (W m^{-2} K), the right-hand term of Eq. (1) becomes $h_r(T_w - T_c)$. Thus, h_r and T_g are expressed as follows:

$$h_r = \sigma\epsilon(T_c + T_w)(T_c^2 + T_w^2) \quad (2)$$

$$T_g = T_c + (T_c - T_w)h_r/h_c \quad (3)$$

In this study, the temperature of the gas was calibrated by this method.

3. Results and discussion

3.1. 5 kW IIR-MCFC stack

The performance of each cell in the 5 kW, IIR-MCFC stack under a current density of 150 mA cm^{-2} is presented in Fig. 3. The average cell voltage was 774 mV and the stack output power was 5.85 kW. As shown in Fig. 3, some cells (e.g., numbers 7, 8 and 14) exhibited inferior performance. This could be caused by poor fuel distribution, because these cells were located next to the RUs.

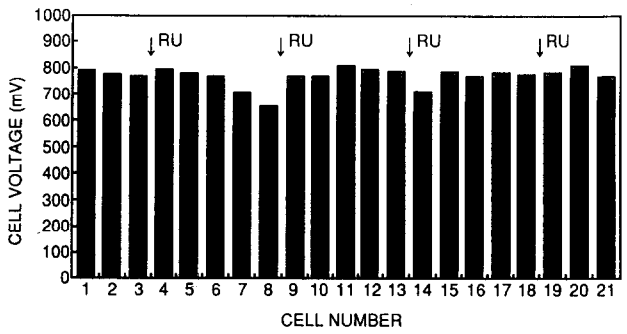

Fig. 3. Performance of each cell in the 5 kW IIR-MCFC stack under a current density of 150 mA cm^{-2}. The fuel was CH_4, the fuel utilization was 72%, the oxidant was air/CO_2 = 70/30, and the oxidant utilization was 30%.

3.1.1. Material-balance study

Fig. 4 gives the results from a material-balance study of the 5 kW IIR-MCFC stack. CH_4 was used as a fuel, the fuel utilization was 72.6%, the steam-to-carbon ratio was 3.6, and the oxidant utilization was 30%. The inlet gas flow rate was controlled by a thermal mass-flow controller, and the water flow rate was controlled by a constant flow-rate water pump. The outlet gas composition was measured by gas chromatography, and the outlet flow rate was calibrated by a tracer gas. Gas which leaked across the matrix from the cathode to the anode was estimated from measurement of content at the anode outlet. The estimated CH_4 flow rate at the anode inlet (which was calculated from the anode outlet H_2-based conversion) became 12.64 mM/S. This almost corresponded to the anode inlet CH_4 setting flow rate of 13.54 mM/S. The estimated flow rate was slightly smaller than the set value because there was some gas leakage from the manifold and, in this calculation, the cross over was estimated only from the cathode to the anode. It was possible, therefore to estimate the material balance by this method.

3.1.2. Heat-balance study

The heat balance around the stack was evaluated by the following relationship:

$$(Q_{cell} - Q_E + Q_X) - Q_{ref} + (Q_{A\,in} - Q_{A\,out}) + (Q_{C\,in} - Q_{C\,out}) + Q_H - Q_{loss} = 0 \quad (4)$$

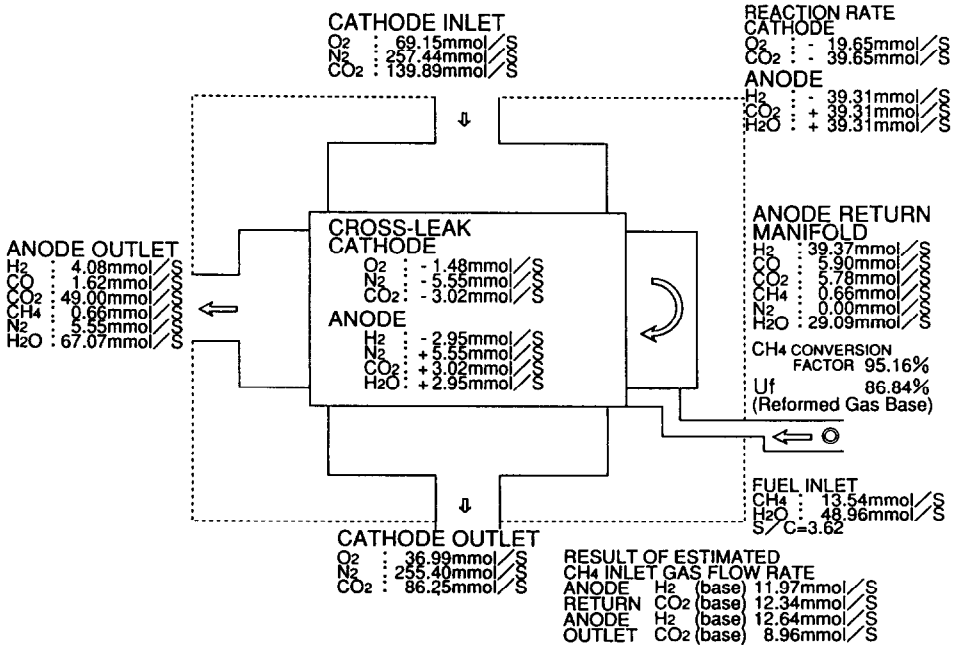

Fig. 4. Results of the material-balance study of the 5 kW IIR-MCFC stack with CH_4 as the fuel. The stack was operated at the current density 150 mA cm^{-2}, the fuel utilization was 72.6%, the steam-to-carbon ratio was 3.6, and the oxidant utilization was 30%.

where Q_{cell} is the heat flux from the cell reaction, Q_E is the output power of the stack, Q_X is the heat flux from gas cross-over inside the stack, Q_{ref} is the heat flux from the reforming reaction, $Q_{A\,in}$ is the heat flux from the anode inlet gas, $Q_{A\,out}$ is the heat flux from the anode outlet gas, $Q_{C\,in}$ is the heat flux from the cathode inlet gas, $Q_{C\,out}$ is the heat flux from the cathode outlet gas, Q_H is the heat flux from the stack electric heater, and Q_{loss} is the thermal radiation from the stack.

3.1.3. Cell reaction and gas cross over

Cell reaction and H_2 and O_2 combustion by gas cross over take place by chemical reactions. The formation of water from H_2 and O_2 is given by:

$$H_2 + 0.5O_2 \longrightarrow H_2O \tag{5}$$

Thus, the heat flux from the cell reaction depends on the hydrogen fraction consumed by the cell reaction and depends on the current. The heat flux is expressed by using the enthalpy of the reaction as follows:

$$Q_{cell} - Q_E = \Delta H Y_{H_2} - Q_E \tag{6}$$

where Y_{H_2} is the fraction of hydrogen consumed by the cell reaction. The heat flux by the gas cross over is given by:

$$Q_X = \Delta H Y_X \tag{7}$$

where Y_X is the fraction of hydrogen consumed by the gas cross over.

3.1.4. Reforming reaction

CH_4 was used as a fuel. Thus, the reforming reaction, that includes the shift reaction, is:

$$CH_4 + 2H_2O \longrightarrow CO_2 + 4H_2 \tag{8}$$

To evaluate the heat flux by the reforming reaction, the enthalpy of CO_2, H_2, CH_4 and H_2O are expressed as follows:

$$Q_{ref} = (\Delta H_{CO_2} + 4\Delta H_{H_2} - \Delta H_{CH_4} - 2\Delta H_{H_2O}) Y_{CH_4} \eta_{CH_4} \tag{9}$$

where Y_{CH_4} is the CH_4 fraction fed to the stack and η_{CH_4} is the reforming coefficient.

3.1.5. Heat flux by each gas

The heat flux by each gas that comes in and goes out of the stack is expressed by:

$$Q_{A\,in} = \sum (C_{p_i} Y_i) T_{A\,in}, \quad i = CH_4, H_2O \tag{10}$$

$$Q_{A\,out} = \sum (C_{p_i} Y_i) T_{A\,out}, \quad i = H_2, CO_2, H_2O, CO, CH_4, N_2 \tag{11}$$

$$Q_{C\,in} = \sum (C_{p_i} Y_i) T_{C\,in}, \quad i = O_2, N_2, CO_2 \tag{12}$$

$$Q_{C\,out} = \sum (C_{p_i} Y_i) T_{C\,out}, \quad i = O_2, N_2, CO_2 \tag{13}$$

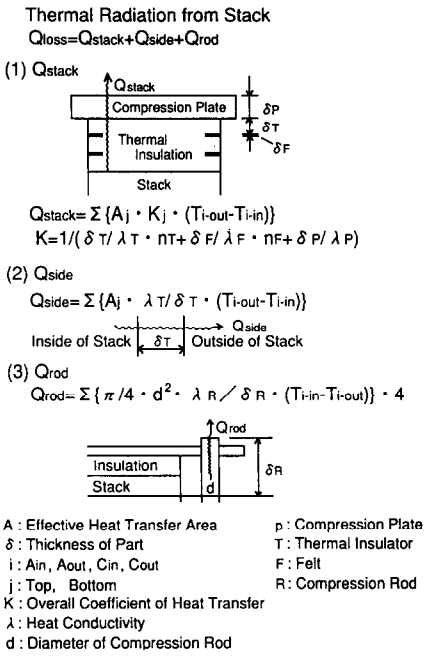

Fig. 5. Method used to evaluated thermal radiation from the stack.

where C_p is the heat capacity of each gas and T is the gas temperature. At the anode outlet, N_2 is by gas cross over.

3.1.6. Thermal radiation from the stack

To evaluate the thermal radiation from the stack, Q_{loss}, three terms were taken into account, as shown in Fig. 5. These terms are: Q_{stack} heat loss from the stack such as compression plate: Q_{side} stack side thermal insulation wall, and Q_{rod} stack compression rods. The Q_{loss} is expressed as:

$$Q_{loss} = Q_{stack} + Q_{side} + Q_{rod} \tag{14}$$

where

$$Q_{stack} = \sum (A_j K_j (T_{i-out} - T_{i-in})) \tag{12}$$

$$Q_{side} = \sum (A_j \lambda_T / \delta_R (T_{i-out} - T_{i-in})) \tag{13}$$

and

$$Q_{rod} = \sum (\pi / 4 d^2 \lambda_R / \delta_R (T_{i-out} - T_{i-in})) 4, \tag{14}$$

$$i = A_{in}, A_{out}, C_{in}, C_{out}, \text{ and } j = \text{top, bottom}$$

where A is the effective heat-transfer area, δ the thickness, λ the heat conductivity, d the diameter of the compression rod, and K is the overall coefficient of heat transfer and is given by:

$$K = 1/(\delta_T/\lambda_T n_T + \delta_F/\lambda_F n_F + \delta_P/\lambda_P) \tag{15}$$

where n is the number part, and subscript P is for the compression plate, T for the thermal insulator, F for the felt, and R for the compression rod.

3.1.7. Heat balance of the stack

Table 4 presents a summary of the heat balance both measured and calculated by the above method. For example, when the fuel utilization is 40% and the oxidant utilization is 30%,

Table 4
Summary of heat-balance study of 5 kW IIR-MCFC stack

U_f (%)	40	50	55	60	60
U_{ox} (%)	30	30	30	30	40
$Q_{A\,in}$ (kW)	2.90	2.21	2.02	1.84	1.84
$Q_{A\,out}$ (kW)	6.84	5.86	5.78	5.19	5.42
$Q_{C\,in}$ (kW)	14.84	14.98	14.46	14.82	10.90
$Q_{C\,out}$ (kW)	13.53	13.55	12.70	12.90	10.20
Q_{cell} (kW)	9.72	9.72	9.73	9.73	9.73
Q_e (kW)	6.19	6.13	6.04	5.85	5.90
Q_{ref} (kW)	3.60	2.78	2.63	2.45	2.51
Q_H (kW)	1.08	0.32	0.39	0.23	0.01
Q_X (kW)	0.91	0.79	0.87	0.73	0.87
Q_{loss} (kW)	0.52	0.52	0.52	0.52	0.53
Q_{in} (kW)	29.45	28.04	27.47	27.35	23.35
Q_{out} (kW)	30.68	28.83	27.66	26.91	24.56

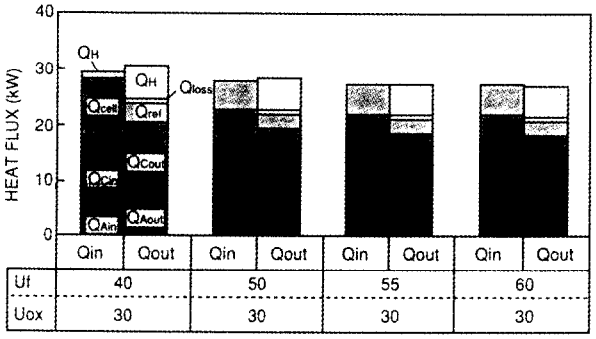

Fig. 6. Contribution of each heat flux around the 5 kW IIIR-MCFC stack.

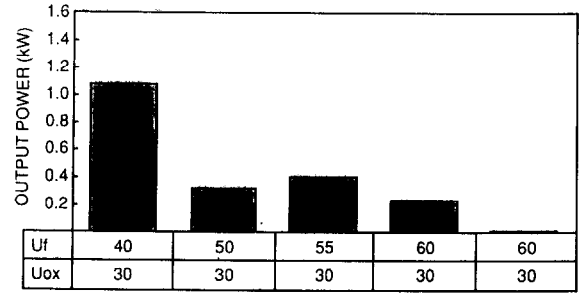

Fig. 7. Mean output power of an electric heater in 5 kW IIR-MCFC.

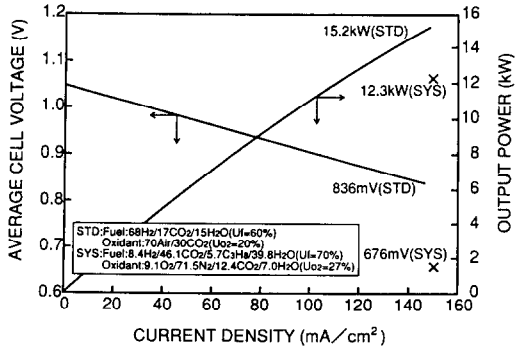

Fig. 8. Voltage–current and power characteristics of the 10 kW, DIR-MCFC. Under standard gas condition, the utilization is 60% and the oxidant utilization is 20%. The system gas condition fuel utilization is 70% for the stack and 80% for the system, while the oxidant utilization is 27% for the stack and 60% for the system.

both the input and the output heat are almost equal, namely; 29.45 and 30.68 kW, respectively. In other cases, such as a fuel utilization of 50, 55 and 60%, the error for input and output heat values is less than 5%. Therefore, it appears to be possible to evaluate the heat balance by the method used in this study.

Fig. 6 shows the contribution of each heat flux around the stack. As the fuel utilization increases, the heat flux contributed by the anode gas becomes lower. The anode inlet gas contributes about 8% of the total inlet heat flux, while the anode outlet gas contributes 21% of the total outlet heat flux. The latter is 2.6 times that of the inlet heat flux, and it corresponds to the volume change of the anode gas that is caused by both the reforming reaction and the cell reaction. The cathode sides contribute about 50% of the inlet and the outlet total heat flux. So it appears easy to control the stack temperature by controlling the gas flow rate of the cathode side. For each fuel utilization, the heat from the cell reaction is almost the same, i.e. 9.7 kW, because the current density is constant at 150 mA cm^{-2}.

Fig. 7 shows the mean output power of the stack's electric heater. As the fuel utilization increases, the mean output power decreases. For a fuel utilization of 60% and an oxidant utilization of 40%, the mean output power is 0.01 kW. Thus, if the stack is operated at high fuel or oxidant utilizations, the stack has to be cooled in order to maintain the optimum operating temperature. This means that the waste heat can be used for the co-generation system.

3.2. 10 kW DIR-MCFC stack

Fig. 8 shows the current–voltage and power characteristics of the 10 kW DIR-MCFC stack. Under the standard gas condition, the output power was 15.2 kW and the average cell voltage was 836 mV. By contrast, for the system gas condition, the output power was 12.3 kW and the average cell voltage was 676 mV. From these results, when the system gas is used with an anode recycle, and the fuel utilization is 80%, the estimated system efficiency is 50.9%.

3.2.1. Material-balance study

The 10 kW DIR-MCFC stack had a vessel to maintain the pressure of the stack. The pressure of the vessel was higher than that of the MCFC reactant gas at the manifolds. Consequently, the N_2 in the vessel entered the stack through the seal of the manifold, and prevented an exact measurement of the material balance. Thus, for the 10 kW DIR-MCFC stack, the calculation of the material balance was performed by using the stack load current as a tracer.

For the anode, the material balance was expressed as follows:

$$F_{A\,tot} = H_{2R}/(H_{2in} - H_{2out}) \quad (16)$$

where $F_{A\,tot}$ is the anode inlet gas flow rate (converted as H_2 and CO_2), H_{2R} the reactant hydrogen flow rate (calculated

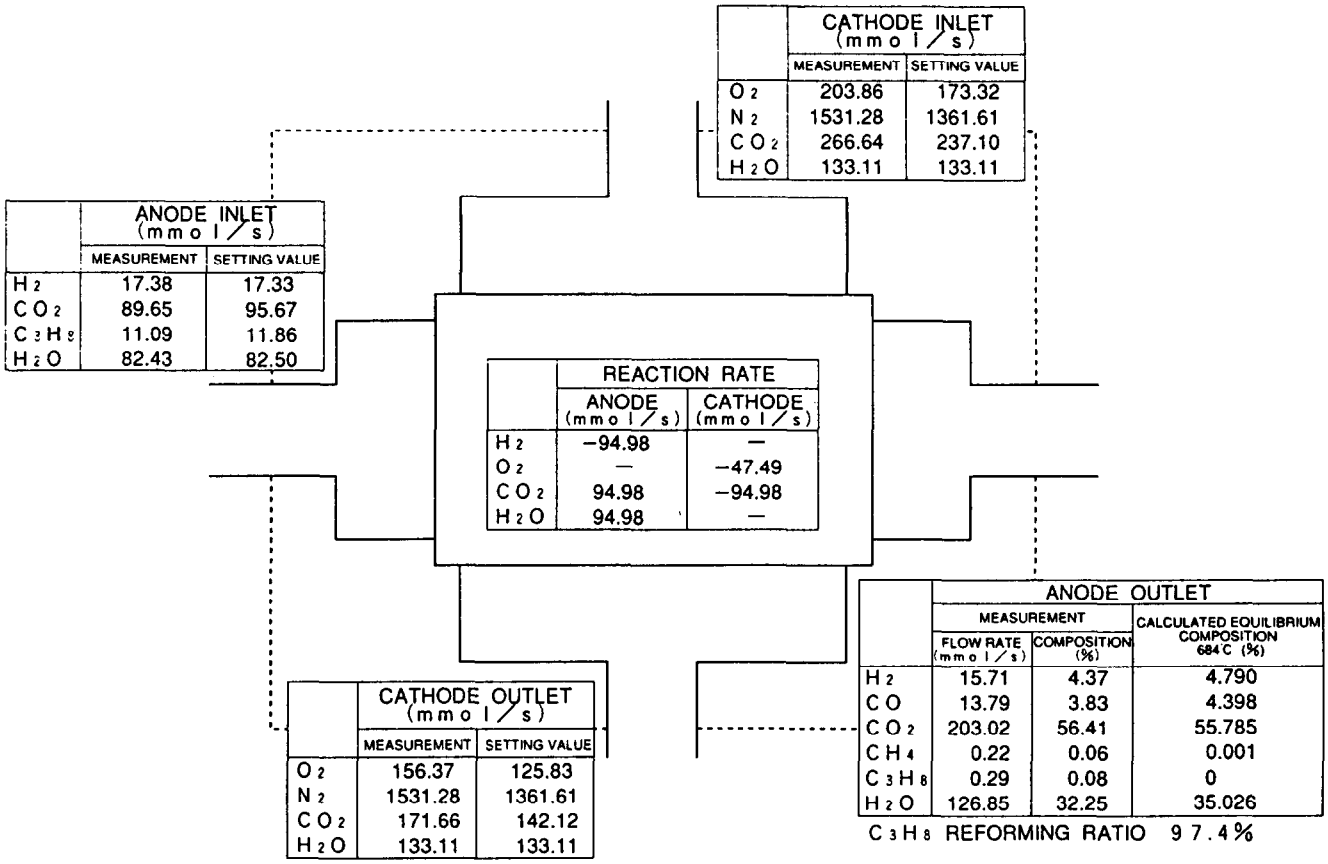

Fig. 9. Material-balance study of the 10 kW DIR-MCFC under the system gas condition.

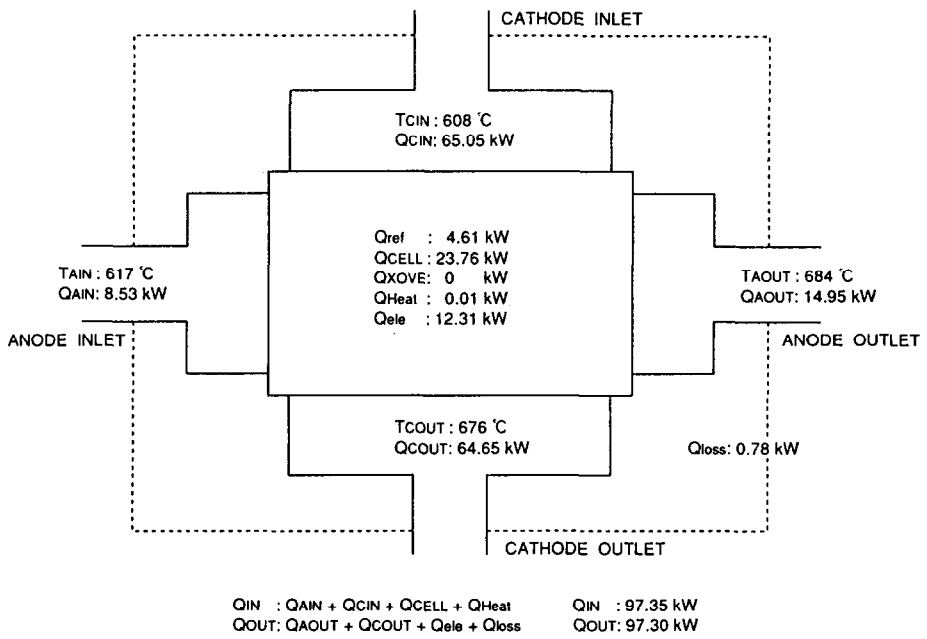

Fig. 10. Heat-balance study of the 10 kW, DIR-MCFC stack under the system gas condition.

from the stack's load current), and $H_{2_{in}}$ and $H_{2_{out}}$ is the H_2 mol fraction at the anode inlet and outlet, respectively.

The material balance for the cathode was calculated in a similar fashion, i.e.,

$$F_{C\,tot} = [(1-O_{2_{out}})O_{2_R}/(O_{2_{out}}+N_{2_{out}})]/ ([O_{2_{in}}/(O_{2_{in}}+N_{2_{in}}) - O_{2_{out}}/(O_{2_{out}}+N_{2_{out}})] \quad (17)$$

where $F_{C\,tot}$ is cathode inlet gas flow rate, O_{2_R} is the reactant

oxygen flow rate calculated from the stack's load current, $O_{2_{in}}$, $O_{2_{out}}$, $N_{2_{in}}$, $N_{2_{out}}$ are the oxygen and the nitrogen contents of the reactant gas at the cathode inlet and outlet, respectively.

Fig. 9 shows the material balance for the 10 kW DIR-MCFC under the system gas condition. As shown in Fig. 9, the inlet and the outlet gas flow rates correspond well to the set value. Moreover, at the anode outlet, the shift equilibrium calculation (at 684 °C) agrees well with the measured gas composition.

3.2.2. Heat-balance study

The heat-balance calculation was performed by the method used above for the 5 kW IIR-MCFC unit. The results are shown in Fig. 10. It can be seen that the input heat was 97.35 kW and the output heat was 97.30 kW. The heat loss was evaluated as 0.8%. This means that the heat loss does not affect the heat balance study. The output power of the stack's electric heater was almost zero. Thus, the stack can operate independently without heat by parastic power.

4. Conclusions

The heat and material balances of the 5 kW IIR-MCFC and the 10 kW DIR-MCFC systems have seen measured. Both stacks exhibit good agreement between the input and output heat. Moreover, both stacks require almost no parastic power for stack heating. This offers the possibility of applying the MCFC as a co-generation system.

Acknowledgements

Part of this work was performed with the support of the PEC (Petroleum Energy Center) Technical Development Division, which is subsidized by MITI.

References

[1] Y. Aoyagi, T. Hashimoto, T. Nishimoto, A. Saiai, Y. Miyake, T. Nakajikma, K. Harima, T. Saitoh, H. Yanaru and H. Fukuyama, *Proc. Int. Fuel Cell Conf., Makuhari, Japan, 3–6 Feb. 1992*, pp. 235–238.

[2] J. Tanaka, A. Saiai, S. Sakurada, T. Nakjima, Y. Miyake, T. Saitoh, M. Sasaki and Y. Yanaru, *Proc. 3rd Symp. Carbonate Fuel Cell Technology, Honolulu, HI, USA, 16–21 May 1993*, pp. 37–47.

[3] S. Sato, Y. Yamaru, A. Saiai and Y. Miyake, *Proc. 1st FCDIC Fuel Cell Symp., Tokyo, Japan, 27–28 June 1994*, pp. 204–209.

[4] T. Saitoh, A. Saiai, S. Sakurada, T. Saitoh and M. Okada, *Program and Abstr., Fuel Cell Seminar, Tucson, AZ, USA, 29 Nov.–2 Dec. 1992*, pp. 77–80.

[5] Y. Miyake, K. Harima, T. Nakajima, N. Nakanishi, T. Saitoh, Y. Aoyagi, J. Tanaka, A. Saiai, H. Yanaru, M. Sasaki and M. Okada, *Proc. 3rd Symp. Carbonate Feul Cell Technology, Honolulu, HI, USA, 16–21 May 1993*, pp. 63–74.